Chilean Journal of Statistics
Vol. 17, No. 1, June/July 2026, 40–67
DOI: 10.32372/ChJS.17-01-03

Parametric Estimation, Censoring, and Survival Analysis
Research Article

An anchor-based conditional framework for interval-censored survival data using a shifted Weibull regression model with mixed covariates

Suman Kapoor[1,*] and Arindam Gupta[1]

[1]Department of Statistics, University of Burdwan, Burdwan, India

(Received: 24 November 2025 · Accepted in final form: 24 February 2026)

Abstract

The three-parameter Weibull distribution is useful in time-to-event analysis because its location can represent a delayed onset of risk or an initial failure-free period when this is scientifically justified. The article develops an anchor-based conditional fitting method for interval-censored survival data under a shifted Weibull accelerated failure time structure with continuous and categorical covariates. The method fixes the location component at an observed design support anchor determined by the lower endpoints of the observed event intervals and then estimates the shape and regression parameters conditionally by the maximum likelihood method. This separates the boundary-sensitive support parameter from the second-stage likelihood optimization and yields interpretable post-anchor shape and covariate effects. We derive the corresponding piecewise interval-censored likelihood and conditional score equations, with explicit treatment of intervals whose lower endpoint lies at or before the anchor. A boundary-calibrated Monte Carlo diagnostic study evaluates root mean squared error, empirical coverage, interval width, convergence, and variance-validity diagnostics for the conditional second-stage estimators when the selected anchor is close to the data-generating endpoint by construction. The method is illustrated using a constructed interval-censored representation of the German Breast Cancer Study Group data and a boundary-stress example based on mice tumor-onset data. The results support the proposed procedure as a design-anchored and numerically stable conditional strategy under the evaluated boundary-calibrated design and near-true initialization for fitting anchored shifted Weibull working models under the interval-censored designs evaluated here.

Keywords: Accelerated failure time model · Boundary nonregularity · Conditional maximum likelihood · Interval censoring · Shifted Weibull distribution.

Mathematics Subject Classification: Primary 62N02 · Secondary 62N01

1. Introduction

Survival analysis provides a statistical framework for studying time-to-event outcomes, such as death, disease recurrence, relapse, recovery, or device failure. In medical studies, the time origin is commonly defined by a clinically meaningful starting point, such as treatment initiation, diagnosis, surgery, or study enrollment [1, 2].

A central feature of survival data is censoring: for some participants, the event time is only partially observed because the study ends before the event occurs, the participant is lost to follow-up, or the event is detected only during scheduled monitoring [1, 3]. These observation patterns require methods designed specifically for censored time-to-event data.

*Corresponding author. Email: skapoor@scholar.buruniv.ac.in (S. Kapoor)

In longitudinal and clinical follow-up studies, the exact event time is often unavailable. Instead, the data may indicate that the event occurred between two assessment times. This setting is known as interval-censored (IC) survival data [4, 5]. IC data arise naturally when participants are examined periodically rather than continuously, as in cancer recurrence studies, screening programs, infection studies, and chronic disease monitoring. The likelihood contribution is then based on the probability that the event time lies within an observed interval, rather than on the probability density function (PDF) at an exactly observed failure time. Parametric survival models are useful when a distributional form is scientifically plausible and direct regression interpretation is desired. The two-parameter Weibull model is widely used because it can represent increasing, decreasing, or constant hazard patterns. A shifted, or three-parameter, Weibull model extends this flexibility by introducing a location component that sets the lower endpoint of the event-time distribution. In this article, the term generalized Weibull model (GWM) refers specifically to this shifted three-parameter Weibull model [6].

The location component of the GWM is scientifically appealing in applications where the observed process suggests a delayed onset of risk. It is also statistically delicate. In exact-observation settings, joint maximum likelihood estimation (JMLE) of the location, shape, scale, and regression parameters can be non-regular in important regions of the parameter space, and standard maximum likelihood (ML) estimation regularity conditions may fail [7, 8]. In IC settings, the likelihood function is based on interval probabilities, but the support endpoint remains closely tied to the inspection schedule and early event intervals. This motivates a fitting strategy that treats the location component as a design-based support anchor and focuses likelihood inference on the remaining model parameters.

This article proposes an anchor-based conditional fitting strategy for IC data with mixed covariates. The location component is fixed at an observed design-based support anchor determined by the lower endpoints of the event intervals. Conditional on this anchor, the shape parameter and regression coefficients are estimated by the ML method. The resulting estimates describe post-anchor survival behavior under the anchored GWM and are interpreted as conditional, or pseudo-true, parameters relative to the selected support endpoint. The anchor is not treated as a regular ML estimator of a latent onset time.

The proposed framework is developed under an accelerated failure time (AFT) regression structure with both continuous and categorical covariates. Its finite-sample behavior is examined through a focused boundary-calibrated Monte Carlo diagnostic study. The simulation evaluates root mean squared error (RMSE), empirical coverage probability (CP), average confidence interval width (ACIW), convergence rate, and variance-validity diagnostics for the conditional second-stage parameters. These summaries assess the conditional performance of the method under the boundary-calibrated design used in the simulation.

The implementation is illustrated using a constructed IC representation of the German Breast Cancer Study Group (GBSG) data [9]. The recorded recurrence-free survival times are converted into event intervals through prespecified follow-up windows, allowing the anchored GWM to be fitted and compared across window choices. The analysis demonstrates the conditional likelihood implementation, the AFT interpretation of covariate effects, and the stability of the main regression conclusions under the evaluated interval constructions.

The remainder of this article is organized as follows. Section 2 reviews the IC structure, introduces the shifted Weibull model, and develops the proposed anchor-based conditional likelihood and score equations. In Section 3, we describe the boundary-calibrated Monte Carlo diagnostic design and performance metrics. In Section 4, the Monte Carlo diagnostic results are reported. Section 5 illustrates the method on a constructed IC representation of the GBSG recurrence data. In Section 6, we provide the conclusions of the present work. Further details on diagnostics, non-regularity, joint-likelihood fits, and illustrations are presented in Appendices A, B, C, and D.

2. Model formulation and anchor-based conditional estimation

2.1 *Abbreviations*

The abbreviations used throughout the article are listed in Table 1.

Table 1. Abbreviations used throughout the article.

Abbreviation	Meaning
ACIW	Average confidence interval width
AFT	Accelerated failure time
AIC	Akaike information criterion
BIC	Bayesian information criterion
BFGS	Broyden–Fletcher–Goldfarb–Shanno
CDF	Cumulative distribution function
CP	Coverage probability
GBSG	German Breast Cancer Study Group
GWM	Generalized Weibull model
IC	Interval-censored
JMLE	Joint maximum likelihood estimation
L-BFGS-B	Limited-memory BFGS with box constraints
ML	Maximum likelihood
PDF	Probability density function
RC	right-censoring
RMSE	Root mean squared error
SE	Standard error

2.2 *Censoring structure and modeling context*

Censoring is a central feature of survival analysis. For the i-th participant, the event time may be observed exactly, partially observed, or not observed during follow-up. Right censoring (RC) occurs when the participant remains event-free up to the last recorded time, whereas IC occurs when the event is known to have occurred between two assessment times. These observation patterns are common in medical studies because of administrative study termination, loss to follow-up, treatment withdrawal, and periodic monitoring [3, 10]. Competing clinical events require additional assumptions and, in general, should not be treated as ordinary non-informative censoring unless a suitable competing-risks or independent-censoring justification is provided.

For IC data, the observed event information is represented by an interval $(L, R]$, where L and R are the lower and upper assessment times. Thus, the event occurred after L and no later than R. Left-censored observations can be represented as IC observations with lower endpoint zero, while RC observations are represented by a last event-free time and an unobserved upper endpoint. Because IC likelihood contributions are based on interval probabilities, the analysis differs from the exact-event-time setting [4]. The likelihood function developed in this article is written for IC event observations and RC observations. Exactly observed failure times are not part of the main data structure used below. If exact failures were present, their likelihood contribution would have to be added through the PDF $f_i(t)$. In our development and applications, exact event times are either absent or deliberately converted into constructed event intervals.

Early non-parametric work on censored survival data includes the estimator proposed by Turnbull [5]. Later developments considered smoothing methods, PDF estimation, and extensions to more complex censoring and truncation structures [11, 12]. These methods provide important non-parametric foundations for IC data, while regression modeling often requires additional structure to describe covariate effects.

Survival models for censored data are grouped into non-parametric, semi-parametric, and parametric approaches [13]. Non-parametric methods are useful when the objective is to estimate the survival distribution with relatively weak structural assumptions.

Semi-parametric methods provide flexible regression formulations, while parametric models specify a full distribution for the survival time and can offer direct interpretation of distributional parameters and covariate effects. The choice among these approaches depends on the scientific question, the censoring mechanism, the available follow-up structure, and the suitability of the distributional assumptions.

Within the parametric class, the exponential distribution provides a simple baseline model, but its constant-hazard structure can be restrictive when the event risk changes over time. Generalized exponential models for IC regression with covariates have been studied in [14, 15]. The present article considers a shifted Weibull formulation instead. The Weibull family is attractive in survival analysis because its shape parameter can represent increasing, decreasing, or constant hazard patterns, making it suitable for applications in which the risk profile changes over follow-up.

2.3 *Shifted Weibull model*

The GWM, as used in this article, refers to the shifted three-parameter Weibull model with location, scale, and shape components [6]. This terminology is used as an article-specific label for the shifted Weibull model considered here. It is not intended to cover all distributions that have been called generalized Weibull distributions in the broader lifetime-distribution literature. The location component determines the lower endpoint of the region in which the PDF is positive. In applications involving latency, delayed disease onset, or engineering systems with an initial protected period, this component can be used to represent the endpoint of an initial failure-free interval, when such an interpretation is scientifically appropriate. Weibull-type generalizations and applications have also been discussed in the broader lifetime-distribution literature [16].

Let T denote the event time. For $c > 0$, $\sigma > 0$, and $\mu \geq 0$, the cumulative distribution function (CDF) of the shifted Weibull model is given by

$$F(t;\mu,\sigma,c) = \begin{cases} 0, & t \leq \mu; \\ 1 - \exp\left(-\left(\dfrac{t-\mu}{\sigma}\right)^{c}\right), & t > \mu. \end{cases} \tag{1}$$

The corresponding survival function is stated as

$$S(t;\mu,\sigma,c) = 1 - F(t;\mu,\sigma,c) = \begin{cases} 1, & t \leq \mu; \\ \exp\left(-\left(\dfrac{t-\mu}{\sigma}\right)^{c}\right), & t > \mu. \end{cases} \tag{2}$$

For $t > \mu$, the PDF is defined as

$$f(t;\mu,\sigma,c) = \frac{c}{\sigma}\left(\frac{t-\mu}{\sigma}\right)^{c-1} \exp\left(-\left(\frac{t-\mu}{\sigma}\right)^{c}\right), \quad t > \mu. \tag{3}$$

For $t < \mu$, the PDF is zero. The value at the single point $t = \mu$ is immaterial for likelihood calculations because the distribution has no point mass at the location endpoint.

For $t > \mu$, the hazard function is established as

$$h(t;\mu,\sigma,c) = \frac{c}{\sigma}\left(\frac{t-\mu}{\sigma}\right)^{c-1}, \quad t > \mu. \tag{4}$$

For $t < \mu$, the hazard is taken to be zero because the event cannot occur before the support endpoint. The right-hand boundary behavior at $t = \mu$ depends on c: the hazard limit is infinite for $0 < c < 1$, finite for $c = 1$, and zero for $c > 1$.

Expressions presented in (1), (2), (3), and (4) define the shifted Weibull distribution used throughout the article. The piecewise survival function given in (2) is especially important for IC likelihood construction, because an observed interval may have a lower endpoint $L_i \leq \mu$. In that case, the correct left-endpoint contribution is $S(L_i) = 1$, and no expression involving $L_i - \mu$ is evaluated.

The location component of the GWM requires careful treatment in likelihood-based inference. For exact event times, the three-parameter Weibull likelihood function has well-known non-regular features in boundary-sensitive shape regimes [7, 8]. For IC data, the likelihood function is constructed from interval probabilities, but the support endpoint remains influenced by the observed inspection intervals. This motivates the anchor-based conditional approach developed below: the location component is fixed at an observable event-interval anchor, and the remaining shape and regression parameters are estimated conditionally.

2.4 *Anchor-based conditional estimation*

The proposed method uses a conditional estimation strategy for the shifted Weibull regression model. The support endpoint is first fixed at a design-based anchor determined by the observed event intervals. Conditional on this fixed anchor, the shape parameter and regression coefficients are estimated by the ML method. This separates the boundary-sensitive support endpoint from the second-stage likelihood optimization and gives the fitted model a direct interpretation as an anchored GWM. The regression structure is specified through a multivariable AFT formulation with both continuous and categorical covariates, extending IC regression settings such as those considered in [14].

Step 1: Design-based anchor for the location component. Assume that at least one IC event observation is available. Let I denote the set of participants with observed IC event intervals. The design-based anchor is defined as

$$I = \{i\colon \delta_{I_i} = 1\}, \quad \widehat{\mu}_A = \min_{i \in I}\{L_i\}. \tag{5}$$

In this framework, $\widehat{\mu}_A$ is an observed design-based support anchor. It is determined by the interval construction and by the inspection schedule, rather than by unconstrained maximization of the likelihood function. Therefore, $\widehat{\mu}_A$ should not be interpreted as a regular ML estimator of a latent biological onset time or as a direct estimate of an unknown failure-free period. It defines the lower endpoint of the fitted anchored working model.

Since every valid event interval satisfies $L_i < R_i$, the anchor stated in (5) satisfies $\widehat{\mu}_A \leq L_i < R_i$ for all $i \in I$. Thus, all event-interval likelihood contributions are well defined under the anchored model. If early event intervals have lower endpoint zero, then the anchor is zero by construction. In that case, the model is anchored at the beginning of the recorded time scale, and no biological latency interpretation is implied.

The second-stage estimates obtained below are conditional on this selected anchor. They describe the shape and covariate effects of the post-anchor shifted Weibull working model, not the joint ML estimates of a fully latent three-parameter Weibull model.

Step 2: Conditional ML estimation of shape and regression parameters. Conditional on the fixed anchor $\widehat{\mu}_A$, the individual-specific Weibull scale parameter is modeled through the AFT specification

$$\sigma_i = \exp(b_0 + b_1 x_i + b_2 z_i), \tag{6}$$

where x_i is a continuous covariate and z_i is a categorical covariate. Equivalently, with $\eta_i = b_0 + b_1 x_i + b_2 z_i$, so that $\sigma_i = \exp(\eta_i)$.

For the score derivations, define the inverse scale parameter as

$$\beta_i = \frac{1}{\sigma_i} = \exp(-\eta_i). \tag{7}$$

Let $\boldsymbol{b} = (b_0, b_1, b_2)^\top$ and $w_{i0} = 1$, $w_{i1} = x_i$, and $w_{i2} = z_i$. From the formulation established in (7), we have that $\partial\beta_i/\partial b_j = -\beta_i w_{ij}$, for $j = 0, 1, 2$. The AFT parametrization stated in (6) guarantees $\sigma_i > 0$ and gives a time-scale interpretation to the regression coefficients.

2.5 *Conditional likelihood for interval-censored data*

For each participant, the observed data are represented either by an RC observation or by an IC event interval. Let $\delta_{R_i} = 1$ denote RC at L_i, and let $\delta_{I_i} = 1$ denote an event observed in $(L_i, R_i]$. In the data structure considered here, $\delta_{R_i} + \delta_{I_i} = 1$.

For fixed $\widehat{\mu}_A$, define the anchored cumulative hazard contribution as

$$V_{i,t}(\widehat{\mu}_A) = \begin{cases} (\beta_i(t - \widehat{\mu}_A))^c, & t > \widehat{\mu}_A; \\ 0, & t \leq \widehat{\mu}_A. \end{cases} \tag{8}$$

The corresponding individual survival function is stated as $S_i(t; \widehat{\mu}_A, c, \boldsymbol{b}) = \exp\left(-V_{i,t}(\widehat{\mu}_A)\right)$. The conditional likelihood function is given by

$$L(c, \boldsymbol{b}; \widehat{\mu}_A) = \prod_{i=1}^{n} \left(S_i(L_i)^{\delta_{R_i}} (S_i(L_i) - S_i(R_i))^{\delta_{I_i}} \right), \tag{9}$$

and the corresponding conditional log-likelihood function is defined as

$$\ell(c, \boldsymbol{b}; \widehat{\mu}_A) = \sum_{i=1}^{n} \left(\delta_{R_i} \log\left(S_i(L_i)\right) + \delta_{I_i} \log\left(S_i(L_i) - S_i(R_i)\right)\right). \tag{10}$$

The likelihood function presented in (9) assumes that the observation consists of RC observations and proper event intervals with $L_i < R_i$. Exact event contributions are not included in (9). Thus, the formula should not be applied unchanged to datasets containing exact failures coded as $L_i = R_i$. The likelihood function is interpreted conditionally on the observed inspection intervals and censoring indicators. As in standard parametric analyses of IC data, this requires that the observation process be non-informative for the event-time distribution after conditioning on the included covariates. If the visit process, censoring process, or interval construction depends on the unobserved event time in an informative way, the likelihood function stated in (9) should be interpreted as a working likelihood function rather than as the full data-generating likelihood function. The expressions defined in (8), (9), and (10) automatically handle event intervals with $L_i \leq \widehat{\mu}_A$, including left-censored intervals with $L_i = 0$. In this case, the left-endpoint cumulative hazard is zero and $S_i(L_i) = 1$. Hence, the interval contribution becomes $1 - S_i(R_i)$, while the right endpoint remains active in the likelihood function.

The conditional likelihood function established in (9) is a product of probabilities. Therefore, it is bounded between 0 and 1. The log-likelihood function presented in (10) is optimized over c and $\boldsymbol{b}$, conditional on $\widehat{\mu}_A$. Numerical safeguards are used to flag invalid floating-point evaluations while preserving the likelihood definition expressed in (9).

2.6 *Conditional score equations*

The second-stage conditional estimates are obtained by solving the score equations for $\theta = (c, \boldsymbol{b}^\top)^\top$, treating $\widehat{\mu}_A$ as fixed. Using $V_{i,t}$ from the formulation defined in (8), for $t > \widehat{\mu}_A$, we have that $\partial V_{i,t}/\partial c = V_{i,t} \log(\beta_i(t - \widehat{\mu}_A))$. Define $D_{i,t}^{(c)} = V_{i,t} \log(\beta_i(t - \widehat{\mu}_A))$, for $t > \widehat{\mu}_A$. For $j = 0, 1, 2$, we get $\partial V_{i,t}/\partial b_j = -cw_{ij} V_{i,t}$, for $t > \widehat{\mu}_A$. The derivative of the survival function is defined as $\partial S_i(t)/\partial \theta = -\exp(-V_{i,t}) \partial V_{i,t}/\partial \theta$, for $t > \widehat{\mu}_A$. The right endpoint of every event interval satisfies $R_i > \widehat{\mu}_A$ from the formulation stated in (5), and so right-endpoint derivatives are well defined for all IC event observations. For the shape parameter, the conditional score derived from the expression given in (10) is formulated as

$$\frac{\partial \ell(c, \boldsymbol{b}; \widehat{\mu}_A)}{\partial c} = \sum_{i=1}^{n} \Psi_{i,c},$$

where

$$\Psi_{i,c} = \begin{cases} -D_{i,L_i}^{(c)}, & \delta_{R_i} = 1 \text{ and } L_i > \widehat{\mu}_A; \\ 0, & \delta_{R_i} = 1 \text{ and } L_i \leq \widehat{\mu}_A; \\ \dfrac{-\exp(-V_{i,L_i}) D_{i,L_i}^{(c)} + \exp(-V_{i,R_i}) D_{i,R_i}^{(c)}}{\exp(-V_{i,L_i}) - \exp(-V_{i,R_i})}, & \delta_{I_i} = 1 \text{ and } L_i > \widehat{\mu}_A; \\ \dfrac{\exp(-V_{i,R_i}) D_{i,R_i}^{(c)}}{1 - \exp(-V_{i,R_i})}, & \delta_{I_i} = 1 \text{ and } L_i \leq \widehat{\mu}_A. \end{cases}$$

For each regression coefficient b_j, with $j = 0, 1, 2$, the conditional score derived from the expression established in (10) is expressed as

$$\frac{\partial \ell(c, \boldsymbol{b}; \widehat{\mu}_A)}{\partial b_j} = \sum_{i=1}^{n} \Phi_{i,j},$$

where

$$\Phi_{i,j} = \begin{cases} cw_{ij} V_{i,L_i}, & \delta_{R_i} = 1 \text{ and } L_i > \widehat{\mu}_A; \\ 0, & \delta_{R_i} = 1 \text{ and } L_i \leq \widehat{\mu}_A; \\ cw_{ij} \left(\dfrac{V_{i,L_i} \exp(-V_{i,L_i}) - V_{i,R_i} \exp(-V_{i,R_i})}{\exp(-V_{i,L_i}) - \exp(-V_{i,R_i})} \right), & \delta_{I_i} = 1 \text{ and } L_i > \widehat{\mu}_A; \\ cw_{ij} \left(\dfrac{-V_{i,R_i} \exp(-V_{i,R_i})}{1 - \exp(-V_{i,R_i})} \right), & \delta_{I_i} = 1 \text{ and } L_i \leq \widehat{\mu}_A. \end{cases}$$

These case-wise score definitions follow directly from the piecewise cumulative hazard presented in (8). When $L_i \leq \widehat{\mu}_A$, the derivative of the left-endpoint survival term is zero, while the right endpoint R_i continues to contribute to the interval probability.

The score equations are solved numerically. In this article, the conditional log-likelihood function stated in (10) is optimized using the limited-memory Broyden–Fletcher–Goldfarb–Shanno (BFGS) algorithm with box constraints (L-BFGS-B), with the positivity constraint $c > 0$. The AFT parametrization defined in (6) guarantees positive individual scale parameters. Standard errors (SEs) for c and $\boldsymbol{b}$ are computed from the observed Hessian of the negative conditional log-likelihood function and are reported as conditional second-stage SEs.

3. Boundary-calibrated Monte Carlo diagnostic design

3.1 *Boundary-calibrated data-generating mechanism*

The simulation was designed as a boundary-calibrated diagnostic study for IC survival data. Its purpose was to evaluate the conditional second-stage estimation problem when the design-based anchor established in (5) is close to the data-generating lower endpoint. It was not intended to mimic a natural inspection process in which visit times are generated independently of the latent failure time. Sample size, RC proportion, and hazard shape were varied systematically. For each combination of design factors, $N = 1000$ independent datasets were generated.

For each participant i in a sample of size n, two covariates were generated: (i) a continuous covariate, $x_i \sim \mathrm{N}(0, 1)$; and (ii) a binary categorical covariate, $z_i \sim \mathrm{Bernoulli}(0.5)$.

The individual-specific Weibull scale parameter was generated according to the AFT model formulated in (6). Given the data-generating lower endpoint μ, shape parameter c, and scale σ_i, a uniform random variable $U_i \sim \mathrm{U}(0, 1)$ was generated, and the failure time was obtained by inverse transform sampling: $T_i = \mu + \sigma_i(-\log(U_i))^{1/c}$. Because U_i and $1 - U_i$ have the same uniform distribution, this expression is equivalent to the usual inverse-CDF construction for the shifted Weibull model presented in (1). In the simulation, μ defines the lower endpoint of the data-generating event-time distribution. In the fitted model, the support endpoint is represented by the design-based anchor defined in (5), and the shape and regression parameters are estimated conditionally.

For each simulated dataset, a censoring-classification threshold T_C was defined as the empirical $(1 - \mathrm{RC})$-quantile of the generated failure times, where RC denotes the target RC proportion. This threshold is an artificial calibration device used to obtain the desired proportion of RC observations within each simulation setting. It is not interpreted as an independently generated administrative end-of-study time. The observed data for each participant were generated as follows:

- RC observations. If $T_i > T_C$, the observation was recorded as RC at $L_i = T_C$, with $R_i = \infty$ and $\delta_{R_i} = 1$.
- IC observations. If $T_i \leq T_C$, an interval was generated around the failure time. A random interval width W_i was drawn from $W_i \sim \mathrm{U}(0.1T_i, 0.5T_i)$. The event interval was then constructed as $L_i = \max\{\mu, T_i - W_i/2\}$ and $R_i = T_i + W_i/2$, with $\delta_{I_i} = 1$.

Because the event intervals are constructed around the latent failure times, this mechanism deliberately ties the observed interval endpoints to T_i. This choice is useful for a boundary-calibrated diagnostic because it controls the distance between the observed event lower endpoints and the true data-generating support endpoint. However, it does not represent a natural IC mechanism based on independent scheduled inspections. Consequently, the simulation results should be interpreted as conditional evidence for the second-stage estimation problem under the controlled boundary-calibrated construction, not as unconditional evidence for arbitrary IC designs.

Under this diagnostic construction, R_i may exceed the calibration threshold T_C for event observations close to T_C. This is not a contradiction because T_C is used only to classify observations as RC or event-observed in the diagnostic design. It is not a literal maximum follow-up time. This construction creates event intervals whose lower endpoints respect the data-generating support endpoint. As a result, the anchor given in (5) is close to the effective lower endpoint in the generated samples. Therefore, the simulation focuses on the conditional behavior of the second-stage estimators under a controlled boundary-calibrated design. The main simulation design uses event intervals with positive lower endpoints. A complementary boundary-stress illustration with early intervals having lower endpoint zero is presented in Appendix D.

3.2 *Factors, scenarios, optimization, scope, and computational framework*

The simulation varied the following design factors:

- Sample size: $n \in \{30, 50, 80, 100, 150, 200\}$.
- Target RC proportion: $\text{RC} \in \{0.10, 0.25, 0.40\}$.
- Data-generating parameter values: The lower endpoint and regression coefficients were held fixed across scenarios: $\mu = 2.0, b_0 = 0.5, b_1 = -0.7, b_2 = 1.0$. Under the AFT parametrization, $b_1 = -0.7$ shortens the time scale for larger values of x_i, while $b_2 = 1.0$ lengthens the time scale for participants with $z_i = 1$.
- Shape scenarios: Two values of the Weibull shape parameter were considered:
  — [Scenario 1] $c = 0.8$, corresponding to a decreasing post-location hazard.
  — [Scenario 2] $c = 1.5$, corresponding to an increasing post-location hazard.

The two shape values were selected to represent boundary-sensitive regimes motivated by the exact-data theory discussed in Appendix B.

The Monte Carlo simulations were designed to evaluate the conditional likelihood problem after fixing the support endpoint at the design-based anchor defined in (5). The optimizer was initialized near the true data-generating parameter values. This initialization focuses the simulation on the behavior of the conditional ML estimation problem and on the associated Hessian-based variance calculations.

For the data applications in Section 5, Appendix C, and Appendix D, the anchor-based conditional fits use data-driven initial values. Multi-start optimization is used for the comparative constrained joint-likelihood function fits, where the location component and the remaining parameters are optimized simultaneously. Because only a finite number of starting values is used, these joint fits are not claimed to be guaranteed global ML estimates.

All simulations and data analyses were performed in the R programming environment [17]. Data manipulation and formatting were carried out using the `dplyr` and `tidyr` packages. The conditional likelihood function presented in (10) was optimized using the `optim` function from the base `stats` package with the L-BFGS-B algorithm. The positivity constraint $c > 0$ was imposed during optimization, while the AFT parametrization formulated in (6) guarantees positive individual scale parameters. The GBSG and mice datasets were accessed through the `shrink` and `icenReg` packages, respectively. All scripts were run with explicit random seeds and include `sessionInfo()` output to support reproducibility.

3.3 *Performance metrics and diagnostics*

The performance metrics were computed over $N = 1000$ Monte Carlo replications for each simulation scenario. For the second-stage parameters c, b_0, b_1, and b_2, all summaries require successful optimizer convergence, whereas CP and ACIW additionally require valid Hessian-based variance estimates. The anchor $\widehat{\mu}_A$ is summarized separately because it is the design-based support endpoint defined in (5).

Let $\theta \in \{c, b_0, b_1, b_2\}$ denote one of the second-stage parameters, and let θ_0 denote its true data-generating value. Let $\widehat{\theta}_r$ be the estimate obtained in Monte Carlo replication r. Define $\mathcal{C}$ as the set of Monte Carlo replications in which the L-BFGS-B optimizer successfully converged, with $N_C = |\mathcal{C}|$. Let $\mathcal{V} \subseteq \mathcal{C}$ be the subset of converged replications in which the ordinary inverse of the observed Hessian of the negative conditional log-likelihood function exists, is numerically positive definite, and yields strictly positive and finite variance estimates for all second-stage parameters. Let $N^* = |\mathcal{V}|$.

The RMSE is computed over the converged set $\mathcal{C}$, as it depends only on the successful extraction of point estimates and is given by

$$\mathrm{RMSE}(\widehat{\theta}) = \Big(\frac{1}{N_C}\sum_{r\in\mathcal{C}}\Big(\widehat{\theta}_r - \theta_0\Big)^2\Big)^{1/2}.$$

RMSE combines bias and variability. For the second-stage conditional parameters, decreasing RMSE with increasing sample size indicates that the estimates become more concentrated around their simulation targets under the specified design.

For c, b_0, b_1, and b_2, the comparison with the data-generating parameter values is meaningful in this diagnostic design because the anchor is constructed to be close to the data-generating endpoint. If the selected anchor differs materially from the latent endpoint, the conditional target of the anchored working model need not coincide exactly with the original data-generating parameter vector.

In such cases, RMSE and CP relative to the original generating values should be interpreted with caution. The empirical CP and ACIW require valid SEs. Therefore, they are computed exclusively over the variance-valid subset $\mathcal{V}$. The empirical CP is given by

$$\mathrm{CP}(\theta) = \frac{1}{N^*}\sum_{r\in\mathcal{V}} 1_{\left[\theta_0\in\{\widehat{\theta}_r - 1.96\,\widehat{\mathrm{SE}}(\widehat{\theta}_r),\, \widehat{\theta}_r + 1.96\,\widehat{\mathrm{SE}}(\widehat{\theta}_r)\}\right]},$$

where 1_B is the indicator function of the set B and $\widehat{\mathrm{SE}}(\widehat{\theta}_r)$ is the Hessian-based SE in replication r. These CPs describe the conditional Wald intervals for the second-stage parameters given the fixed anchor, for which the ACIW is defined as

$$\mathrm{ACIW}(\theta) = \frac{1}{N^*}\sum_{r\in\mathcal{V}}\big(\widehat{\theta}_{r,U} - \widehat{\theta}_{r,L}\big),$$

where $\widehat{\theta}_{r,L}$ and $\widehat{\theta}_{r,U}$ are the lower and upper Wald interval limits in replication r. This quantity summarizes the average precision of the conditional Wald intervals.

The anchor $\widehat{\mu}_A$ is summarized separately from the likelihood-estimated second-stage parameters. Because $\widehat{\mu}_A$ is a minimum of observed lower endpoints, it is a design-based statistic rather than a regular ML estimator. The reported root mean squared discrepancy for $\widehat{\mu}_A$ is computed relative to the data-generating endpoint μ only as a diagnostic summary of the boundary-calibrated simulation design. It should not be interpreted as the RMSE of a regular estimator under a standard parametric likelihood theory.

Bootstrap resampling with $B = 100$ replications, utilizing the percentile-interval convention, is used to obtain resampling intervals for $\widehat{\mu}_A$. The reported anchor inclusion rate records the proportion of times the data-generating lower endpoint lies within these resampling intervals, and the anchor resampling width summarizes the corresponding average interval lengths. These quantities are descriptive summaries of the resampling behavior of the design-based endpoint. They must not be interpreted as standard confidence-interval CPs or widths for a regular ML-estimated location parameter.

The convergence rate is defined as the proportion of total Monte Carlo replications ($N = 1000$) in which the L-BFGS-B optimizer reported convergence for the conditional likelihood function stated in (10). The variance-validity rate is defined strictly as the proportion of total Monte Carlo replications ($N = 1000$) yielding a finite, symmetric, numerically positive-definite, and well-conditioned Hessian matrix that permits an ordinary inverse. Replications requiring pseudo-inversion are classified as variance-invalid. Replications outside $\mathcal{C}$ are excluded from RMSE calculations, and replications outside $\mathcal{V}$ are excluded from CP and ACIW summaries for c, b_0, b_1, and b_2. The average penalty count records the mean number of invalid objective-function evaluations per replication. The convergence, variance-validity, and penalty summaries are reported together with the conditional performance measures.

4. Monte Carlo diagnostic results

4.1 *Context*

The results evaluate the conditional behavior of the second-stage estimators after fixing the design-based anchor stated in (5). Because the event intervals are deliberately constructed around the latent failure times, the results should be interpreted as evidence about the controlled anchored likelihood problem, not as evidence of general performance under arbitrary independent inspection schedules.

4.2 *RMSE and coverage probability*

The simulation results for Scenario 1 ($c = 0.8$) and Scenario 2 ($c = 1.5$) are reported for the RMSE in Tables 2 and 3, for the empirical CP in Tables 4 and 5, for the interval-width summaries in Tables 6 and 7, and for computational diagnostics in Table 8. Figures 1, 2, and 3 show the corresponding graphical summaries in Appendix A.

Table 2. RMSE summaries for Scenario 1 ($c = 0.8$).

Quantity	Sample size	Target RC proportion		
	n	10%	25%	40%
$\widehat{\mu}_A$ (anchor)	30	0.003772	0.001449	0.002258
	50	0.000000	0.000000	0.000000
	80	0.000000	0.000000	0.000000
	100	0.000000	0.000000	0.000000
	150	0.000000	0.000000	0.000000
	200	0.000000	0.000000	0.000000
c (shape)	30	0.194177	0.204427	0.277539
	50	0.131651	0.142777	0.176993
	80	0.097864	0.109641	0.137654
	100	0.085182	0.088549	0.116352
	150	0.064396	0.075198	0.097145
	200	0.057054	0.066452	0.081154
b_0 (intercept)	30	0.393855	0.413865	0.411411
	50	0.291674	0.293768	0.314864
	80	0.231913	0.227450	0.246058
	100	0.201858	0.201866	0.226448
	150	0.163609	0.165096	0.192426
	200	0.141740	0.137742	0.149956
b_1 (continuous covariate)	30	0.299660	0.350455	0.393322
	50	0.212711	0.262973	0.293186
	80	0.174237	0.190985	0.218922
	100	0.151521	0.168155	0.191909
	150	0.118699	0.137986	0.154851
	200	0.105211	0.120739	0.137514
b_2 (binary covariate)	30	0.549099	0.624025	0.682271
	50	0.413636	0.442501	0.520264
	80	0.309788	0.344279	0.395992
	100	0.271611	0.293611	0.365884
	150	0.219557	0.253862	0.309959
	200	0.198394	0.214768	0.248728

Tables 2 and 3 show that the root mean squared discrepancy of $\widehat{\mu}_A$ from the data-generating endpoint is zero or near zero in most settings. This behavior is a direct consequence of the boundary-calibrated diagnostic construction: the event-interval lower endpoints are generated to respect the data-generating lower endpoint. Therefore, the anchor in (5) is often close to, or equal to, that endpoint. Accordingly, the anchor summaries should be read as diagnostics of the constructed design, not as evidence that $\widehat{\mu}_A$ is a regular estimator of a latent biological endpoint in general IC data.

For c, b_0, b_1, and b_2, RMSE generally decreases as the sample size increases. This indicates that the conditional estimates become more concentrated around their simulation targets under the evaluated design. For a fixed sample size, RMSE tends to increase as the RC proportion increases, reflecting the expected loss of information due to censoring.

Table 3. RMSE summaries for Scenario 2 ($c = 1.5$).

Quantity	Sample size	Target RC proportion		
	n	10%	25%	40%
$\widehat{\mu}_A$ (anchor)	30	0.027743	0.021986	0.026586
	50	0.007949	0.003771	0.003201
	80	0.000000	0.000000	0.000000
	100	0.000000	0.000000	0.000000
	150	0.000000	0.000000	0.000000
	200	0.000000	0.000000	0.000000
c (shape)	30	0.403673	0.436439	0.479332
	50	0.264828	0.280225	0.338423
	80	0.193304	0.218427	0.247795
	100	0.179410	0.192263	0.218673
	150	0.140283	0.153499	0.160236
	200	0.122942	0.123408	0.147879
b_0 (intercept)	30	0.214158	0.218380	0.229202
	50	0.157619	0.160738	0.170713
	80	0.129623	0.125532	0.132647
	100	0.112879	0.117123	0.118847
	150	0.095299	0.096593	0.099164
	200	0.084064	0.088005	0.087431
b_1 (continuous covariate)	30	0.160760	0.203305	0.224415
	50	0.124186	0.148247	0.168557
	80	0.097289	0.109372	0.134114
	100	0.084551	0.099154	0.118262
	150	0.070324	0.081125	0.093593
	200	0.061212	0.070938	0.080162
b_2 (binary covariate)	30	0.296162	0.341866	0.393938
	50	0.221532	0.257967	0.309517
	80	0.170724	0.189230	0.226161
	100	0.154721	0.174788	0.204218
	150	0.126911	0.140440	0.161108
	200	0.106607	0.125672	0.148092

Table 4. Empirical CP for conditional parameters and anchor inclusion summaries for Scenario 1 ($c = 0.8$).

Quantity	Sample size	Target RC proportion		
	n	10%	25%	40%
$\widehat{\mu}_A$ (anchor inclusion rate)	30	0.999	0.999	0.999
	50	1.000	1.000	1.000
	80	1.000	1.000	1.000
	100	1.000	1.000	1.000
	150	1.000	1.000	1.000
	200	1.000	1.000	1.000
c (Shape)	30	0.941	0.971	0.970
	50	0.953	0.958	0.975
	80	0.958	0.963	0.968
	100	0.961	0.978	0.967
	150	0.960	0.964	0.967
	200	0.954	0.960	0.968
b_0 (intercept)	30	0.916	0.924	0.938
	50	0.915	0.934	0.935
	80	0.928	0.941	0.944
	100	0.933	0.951	0.928
	150	0.936	0.941	0.926
	200	0.945	0.957	0.946
b_1 (continuous covariate)	30	0.915	0.931	0.941
	50	0.949	0.931	0.936
	80	0.936	0.943	0.932
	100	0.933	0.956	0.948
	150	0.944	0.951	0.954
	200	0.949	0.947	0.950
b_2 (binary covariate)	30	0.912	0.930	0.937
	50	0.923	0.944	0.943
	80	0.950	0.946	0.954
	100	0.951	0.958	0.948
	150	0.945	0.947	0.932
	200	0.940	0.950	0.953

Table 5. Empirical CP for conditional parameters and anchor inclusion summaries for Scenario 2 ($c = 1.5$).

Quantity	Sample size	Target RC proportion		
	n	10%	25%	40%
$\widehat{\mu}_A$ (anchor inclusion rate)	30	0.951	0.931	0.950
	50	0.994	0.995	0.989
	80	1.000	1.000	1.000
	100	1.000	1.000	1.000
	150	1.000	1.000	1.000
	200	1.000	1.000	1.000
c (shape)	30	0.951	0.966	0.977
	50	0.953	0.963	0.969
	80	0.947	0.951	0.957
	100	0.940	0.955	0.951
	150	0.944	0.946	0.972
	200	0.926	0.957	0.964
b_0 (intercept)	30	0.906	0.916	0.913
	50	0.931	0.923	0.929
	80	0.932	0.930	0.926
	100	0.927	0.924	0.929
	150	0.920	0.919	0.930
	200	0.924	0.896	0.925
b_1 (continuous covariate)	30	0.936	0.934	0.953
	50	0.921	0.944	0.943
	80	0.943	0.945	0.953
	100	0.938	0.948	0.956
	150	0.942	0.946	0.959
	200	0.934	0.950	0.963
b_2 (binary covariate)	30	0.909	0.925	0.930
	50	0.928	0.931	0.933
	80	0.932	0.940	0.942
	100	0.933	0.940	0.947
	150	0.930	0.948	0.957
	200	0.946	0.943	0.951

Table 6. Average interval-width summaries for Scenario 1 ($c = 0.8$).

Quantity	Sample size	Target RC proportion		
	n	10%	25%	40%
$\widehat{\mu}_A$ (anchor resampling width)	30	0.015911	0.014756	0.016819
	50	0.000550	0.000592	0.000424
	80	0.000107	0.000000	0.000000
	100	0.000000	0.000000	0.000000
	150	0.000000	0.000000	0.000000
	200	0.000000	0.000000	0.000000
c (shape)	30	0.634183	0.746864	0.947269
	50	0.467204	0.550871	0.687427
	80	0.359822	0.425919	0.531934
	100	0.319312	0.375309	0.467025
	150	0.256879	0.305206	0.378453
	200	0.220972	0.261223	0.322299
b_0 (intercept)	30	1.345078	1.467255	1.551512
	50	1.042834	1.110474	1.189356
	80	0.828984	0.866384	0.933150
	100	0.738181	0.775821	0.841064
	150	0.607126	0.632408	0.684293
	200	0.526537	0.548538	0.599475
b_1 (continuous covariate)	30	1.071654	1.265964	1.436746
	50	0.808123	0.943707	1.077058
	80	0.637766	0.728093	0.834895
	100	0.563540	0.651600	0.750893
	150	0.459074	0.524884	0.609403
	200	0.396065	0.454456	0.531534
b_2 (binary covariate)	30	1.931356	2.284597	2.568793
	50	1.491856	1.716657	1.965173
	80	1.180880	1.332506	1.535663
	100	1.051726	1.196256	1.388299
	150	0.862452	0.974796	1.125538
	200	0.748066	0.844785	0.981185

Table 7. Average interval-width summaries for Scenario 2 ($c = 1.5$).

Quantity	Sample size	Target RC proportion		
	n	10%	25%	40%
$\widehat{\mu}_A$ (anchor resampling width)	30	0.133118	0.134823	0.139453
	50	0.029544	0.034790	0.031820
	80	0.004164	0.003800	0.004322
	100	0.000918	0.000657	0.001358
	150	0.000017	0.000006	0.000006
	200	0.000000	0.000000	0.000000
c (shape)	30	1.211723	1.381558	1.622790
	50	0.881079	0.987531	1.185462
	80	0.666416	0.761233	0.899409
	100	0.593532	0.672980	0.789618
	150	0.477657	0.540881	0.635846
	200	0.411593	0.463628	0.549603
b_0 (intercept)	30	0.719120	0.759402	0.809829
	50	0.557660	0.591763	0.622937
	80	0.449886	0.461396	0.493432
	100	0.399068	0.412950	0.443108
	150	0.327418	0.339406	0.361286
	200	0.283533	0.293564	0.310976
b_1 (continuous covariate)	30	0.595194	0.721014	0.857375
	50	0.455354	0.549248	0.645225
	80	0.361979	0.424308	0.507606
	100	0.318129	0.377083	0.456392
	150	0.261356	0.309831	0.368825
	200	0.224704	0.265734	0.319114
b_2 (binary covariate)	30	1.034604	1.238918	1.462341
	50	0.803968	0.950114	1.115319
	80	0.643356	0.736597	0.879987
	100	0.571511	0.660049	0.794421
	150	0.468318	0.541649	0.643849
	200	0.404310	0.467135	0.558236

Table 8. Computational stability diagnostics for the conditional second-stage optimization.

Scenario	Aggregated convergence	Aggregated variance-validity	Average penalties
Scenario 1 ($c = 0.8$)	18000/18000	18000/18000	0.000
Scenario 2 ($c = 1.5$)	18000/18000	18000/18000	0.000

The empirical CPs for c, b_1, and b_2 are generally close to the nominal 0.95 level across the evaluated scenarios. The intercept b_0 shows lower CP in several settings, especially in Scenario 2, indicating that the Hessian-based Wald intervals for the baseline scale parameter are more sensitive in finite samples. The reported CP values for $\widehat{\mu}_A$ are anchor inclusion summaries based on the resampling intervals described in Subsection 3.3.

Each entry presented in Table 8 aggregates all 18 evaluated settings (combinations of sample size $n \in \{30, 50, 80, 100, 150, 200\}$ and target RC proportion RC $\in \{0.10, 0.25, 0.40\}$) within the corresponding scenario. Both convergence and variance-validity rates are reported as the absolute number of successful replications out of the total 18,000 iterations per scenario (18 settings $\times$ 1000 replications). Crucially, the minimum rate across all individual settings was exactly 1000/1000, confirming that no failures were concealed through aggregation. The convergence rate represents successful L-BFGS-B optimization. The variance-validity rate represents the subset of total replications in which the observed Hessian was symmetric, strictly positive definite, and well-conditioned, permitting an ordinary matrix inverse. Average penalties denotes the mean number of invalid objective-function evaluations per replication. In the conditional method, the location component is fixed at the design-based anchor $\widehat{\mu}_A$, and so the reported diagnostics concern only the second-stage optimization over c and $\boldsymbol{b}$.

4.3 *Interval widths and computational stability*

To assess numerical stability and finite-sample precision, we examined convergence rates, variance-validity rates, average confidence interval widths, and penalty counts. These results are presented in Tables 6, 7, and 8.

Across all evaluated sample sizes, censoring proportions, and shape scenarios, the conditional second-stage optimization achieved convergence in all reported settings. The Hessian-based variance extraction was also valid in all reported converged replications, and the average number of invalid-objective penalties was zero. These results support the numerical stability of the conditional likelihood function stated in (10) under the simulation design considered here.

For c, b_0, b_1, and b_2, the ACIW decreases as the sample size increases, reflecting improved precision with larger samples. Conversely, ACIW increases as the right censoring proportion increases, which is consistent with the loss of information caused by heavier censoring. For $\widehat{\mu}_A$, the reported width is the bootstrap resampling-summary width for the anchor.

Overall, the diagnostic study shows that the proposed anchor-based conditional likelihood function can be optimized reliably under the boundary-calibrated construction and near-true initialization evaluated here. When the design-based anchor is close to the data-generating lower endpoint by construction, the second-stage estimates of the shape and regression parameters exhibit decreasing RMSE as sample size increases, stable convergence behavior, and interpretable Hessian-based uncertainty summaries.

These findings support the proposed method as a numerically stable conditional fitting strategy for the anchored shifted Weibull working model under the evaluated boundary-calibrated design and near-true initialization. They should not be generalized without qualification to settings with dispersed starting values, IC data generated by independent inspection schedules, informative visit processes, or other observation mechanisms not studied here.

5. Application to constructed interval-censored GBSG recurrence data

5.1 *Context*

This section illustrates the implementation of the proposed anchor-based conditional method using the GBSG dataset, available through the R package `shrink` [9]. The recorded recurrence-free survival times are converted into constructed IC event intervals under prespecified follow-up-window assumptions. The analysis demonstrates how the anchored GWM can be fitted, how the AFT covariate effects can be interpreted, and how the estimates behave under different interval-window constructions.

5.2 *GBSG data and interval construction*

The GBSG dataset contains information on 686 women with node-positive breast cancer. The variables used in this analysis are as follows. The variable `rfst` is the recurrence-free survival time in days. The variable `cens` is the event indicator, with 0 denoting censoring and 1 denoting recurrence. The variable `age` is the age in years. The variable `htreat` is a binary indicator for hormonal therapy, with 0 denoting no hormonal therapy and 1 denoting hormonal therapy. In the fitted regression model, age is standardized as $x_i = (\mathtt{age}_i - \overline{\mathtt{age}})/s_{\mathtt{age}}$, where $\overline{\mathtt{age}}$ and $s_{\mathtt{age}}$ are the sample mean and sample standard deviation of age in the analyzed dataset. Thus, the coefficient b_1 corresponds to a one-standard-deviation increase in age.

The recorded recurrence-free survival times were converted into IC and RC observations using a prespecified follow-up window. For the primary analysis, a 10-day window was used. This construction defines the observed endpoints as follows:

- Participants with recurrence ($\texttt{cens} = 1$). The recurrence time is $\texttt{rfst}$ and under the 10-day window construction, the event interval is $(L_i, R_i] = (\max\{1, \texttt{rfst} - 10\}, \texttt{rfst}]$.
- Participants without recorded recurrence ($\texttt{cens} = 0$). The observation is treated as RC at the recurrence-free survival time, with $L_i = \texttt{rfst}$ and $R_i = \infty$.

This interval construction is an analytic device used to illustrate the anchored IC likelihood function on a well-known breast cancer dataset. The original recorded rfst values are not treated here as naturally observed inspection intervals with a documented visit schedule. Therefore, the results below should be interpreted as conditional analyses under the constructed IC representations, rather than as direct evidence from a naturally IC GBSG inspection process.

Under the primary 10-day construction, the earliest event lower endpoint is 62 days, obtained from the earliest recorded recurrence time of 72 days. Using the anchor definition in (5), the corresponding design-based anchor for the conditional GWM fit is $\widehat{\mu}_A = 62$.

5.3 *Primary 10-day conditional fit*

The anchored GWM was first compared with the ordinary two-parameter Weibull model under the primary 10-day interval construction. The two-parameter Weibull model fixes the lower endpoint at zero, whereas the anchored GWM fixes the lower endpoint at the 10-day design-based anchor and estimates the shape and regression parameters conditionally.

For this comparison, we report the maximized conditional log-likelihood function together with descriptive quantities in the algebraic form of Akaike information criterion (AIC)-like score and Bayesian information criterion (BIC)-like score. These quantities are not used as ordinary unrestricted model-selection criteria. The reason is that the anchored model fixes $\widehat{\mu}_A$ through a data-dependent design rule rather than estimating it by ordinary likelihood maximization. Consequently, there is no unique standard parameter-count interpretation for AIC-like score or BIC-like score in this conditional anchored comparison.

For transparency, the anchored model is reported with $k = 5$ components, counting the fixed anchor as a descriptive model component, while the two-parameter Weibull model is reported with $k = 4$ components. This choice gives a conservative descriptive penalty to the anchored model. The resulting summaries should be interpreted only as conditional descriptive fit summaries for the constructed 10-day IC representation. Table 9 reports the comparison.

Table 9. Fit comparison for the GBSG data under the primary 10-day interval construction ($n = 686$).

Model	Components (k)	Log-likelihood	AIC-like score	BIC-like score
Weibull ($\mu = 0$)	4	-1943.8	3895.6	3913.7
Anchored GWM ($\widehat{\mu}_A = 62$)	5	-1933.8	3877.5	3900.2

The safest conclusion is that the anchored GWM has a higher maximized conditional log-likelihood than the two-parameter Weibull model under the constructed 10-day representation, while the penalized descriptive scores depend on the chosen counting convention. This indicates that using the observed event lower-endpoint anchor as the fitted support endpoint improves the conditional descriptive fit without treating the ad hoc penalized scores as ordinary model-selection criteria.

5.4 *Conditional parameter estimates*

Table 10 reports the conditional second-stage estimates from the anchored GWM under the primary 10-day interval construction. These estimates are conditional on the design-based anchor $\widehat{\mu}_A = 62$. Table 11 reports the corresponding anchor summary.

Table 10. Second-stage estimates from the anchored GWM under the primary 10-day interval construction.

Parameter	Estimate	SE	Null	z-value	p-value	Lower	Upper
c (shape)	1.1508	0.0579	$c = 1$	2.6045	0.0092	1.0374	1.2642
b_0 (intercept)	7.9331	0.0967	$b_0 = 0$	82.0307	< 0.0001	7.7435	8.1226
b_1 (age, standardized)	-0.0007	0.0532	$b_1 = 0$	-0.0137	0.9891	-0.1050	0.1035
b_2 (hormonal therapy)	0.3355	0.1114	$b_2 = 0$	3.0123	0.0026	0.1172	0.5538

Table 11. Design-based anchor summary for the primary 10-day GBSG construction.

Quantity	Value	Resampling lower	Resampling upper
$\widehat{\mu}_A$	62.0000	62.0000	110.0000

Note: The interval limits represent a resampling-based summary obtained via the percentile-interval convention with B=500 bootstrap replications. Retaining our earlier caution, these are strictly descriptive bounds for the design-based anchor and are not standard confidence intervals for a latent location parameter.

The 10-day construction gives a design-based anchor of 62 days, as shown in Table 11. This value is obtained from the earliest recorded recurrence time of 72 days and the 10-day follow-up window. In the anchored model, it defines the lower endpoint of the fitted support used in the conditional likelihood function. Therefore, it should be interpreted as a design-based support endpoint for the constructed IC representation, not as a direct estimate of a fully latent biological failure-free period.

The estimated shape parameter in Table 10 is greater than 1, and its reported interval lies above 1. Therefore, the Wald statistic for the shape parameter is evaluated against the scientifically relevant null hypothesis H_0: $c = 1$, corresponding to a constant post-anchor hazard. Under the anchored GWM, the result supports an increasing post-anchor recurrence hazard for the primary 10-day construction. The AFT parametrization gives a direct time-scale interpretation to the regression coefficients. The standardized age coefficient is close to zero and is not statistically significant in the primary fit. The hormonal therapy coefficient is positive and statistically significant. Its estimated AFT time-scale multiplier is $\exp(0.3355) \approx 1.40$, indicating that hormonal therapy is associated with a longer post-anchor recurrence-free time scale under the anchored GWM.

5.5 *Sensitivity to the interval window*

To examine the stability of the conditional estimates under different event-interval constructions, the analysis was repeated using 20-day and 30-day windows. Each window produces a corresponding anchored GWM fit through the anchor definition stated in (5). Table 12 reports the resulting anchor values, shape estimates, and regression estimates.

Table 12. Sensitivity of conditional estimates to the constructed interval window.

Quantity	10-day window	20-day window	30-day window
$\widehat{\mu}_A$	62.0000	52.0000	42.0000
$\widehat{c}$	1.1508	1.1600	1.1690
$\widehat{b}_1$ Age	-0.0007	-0.0009	-0.0010
p-value for b_1	0.9891	0.9867	0.9843
$\widehat{b}_2$ hormonal therapy	0.3355	0.3332	0.3311
p-value for b_2	0.0026	0.0026	0.0025

The conditional regression estimates are stable across the three window choices. The age coefficient remains close to zero in all analyses. The hormonal therapy coefficient remains close to 0.33 and statistically significant across all three constructed windows. The corresponding AFT interpretation is consistent across the sensitivity analysis: hormonal therapy is associated with a longer post-anchor recurrence-free time scale under the anchored GWM.

The anchor changes with the chosen interval window, taking values 62, 52, and 42 days for the 10-, 20-, and 30-day constructions, respectively. This behavior follows directly from the interval construction rule and from the anchor defined in (5).

5.6 *Summary of the GBSG application*

The GBSG application demonstrates the practical implementation of the anchor-based conditional GWM for a constructed IC survival dataset. Under the primary 10-day window, the anchored GWM provides an improved conditional descriptive fit relative to the two-parameter Weibull model. The fitted shape parameter indicates an increasing post-anchor hazard, and the AFT regression results show a stable positive association between hormonal therapy and the recurrence-free time scale.

The sensitivity analysis across 10-, 20-, and 30-day windows shows that the main regression conclusions remain stable across the evaluated interval constructions. The changing anchor values reflect the window-specific construction of the event intervals, while the conditional regression estimates remain similar across the evaluated windows.

The analysis supports the practical usefulness of the anchored conditional GWM as a descriptive and regression-oriented tool for shifted Weibull survival modeling with constructed IC observations. A complementary numerical comparison between the anchor-based conditional method and best converged constrained joint fits for the constructed GBSG interval windows is reported in Appendix C. The corresponding location values, shape estimates, and log-likelihood functions are summarized in Table 13.

6. Conclusions

6.1 *Summary and implications*

This article developed an anchor-based conditional framework for fitting the GWM (the shifted three-parameter Weibull model) to IC survival data with mixed covariates. The method fixes the support endpoint at the design-based anchor defined in (5) and then estimates the Weibull shape and regression parameters conditionally by the ML method. This construction provides a stable and interpretable way to fit shifted Weibull regression models when the location component is treated as a boundary-sensitive support parameter.

The main methodological contribution is the separation between the support endpoint and the second-stage likelihood optimization. Conditional on the anchor, the shape and regression parameters are estimated from the IC likelihood function stated in (10). The resulting estimates describe post-anchor survival behavior under the anchored GWM and have a conditional interpretation relative to the selected support endpoint.

The methodological development provided the piecewise IC likelihood function and the corresponding conditional score equations for the shape and regression parameters. The piecewise formulation handles event intervals whose lower endpoint is less than or equal to the anchor, while preserving the right-endpoint contribution to the interval probability. This structure supports direct numerical optimization of the conditional likelihood function and Hessian-based uncertainty summaries for the second-stage parameters.

The Monte Carlo diagnostic study in Sections 3 and 4 showed reliable conditional optimization under the boundary-calibrated construction and near-true initialization considered. Across the evaluated scenarios, the conditional estimates of the shape and regression parameters showed decreasing RMSE as sample size increased, and the convergence and variance-validity diagnostics were stable. These results support the proposed framework as a numerically stable conditional fitting strategy for the anchored shifted Weibull working model under the evaluated boundary-calibrated design and near-true initialization. They do not, by themselves, establish unconditional performance under arbitrary IC mechanisms or independent inspection schedules.

The application to the GBSG data in Section 5 illustrated the implementation of the method using constructed IC recurrence intervals. Because the intervals were created from recorded recurrence-free survival times through prespecified window rules, the analysis should be interpreted as an anchored conditional analysis under constructed interval representations, not as an analysis of a naturally IC inspection schedule. Overall, the proposed approach combines three useful features: a shifted Weibull survival model, a design-based support anchor, and an AFT regression structure for continuous and categorical covariates. Taken jointly, these components provide a flexible and interpretable framework for conditional parametric modeling of IC survival data.

6.2 *Limitations and future research*

Several limitations should be considered when interpreting the results. The anchor defined in (5) is a design-based lower endpoint determined by the observed event intervals. Therefore, its interpretation depends on the inspection schedule, the construction of the interval endpoints, and the time origin used in the study. It is not a regular ML estimator of a latent biological onset time. In datasets with early left-censored intervals, the anchor may be zero. In boundary-calibrated simulation designs, it may be close to the data-generating lower endpoint by construction. Inference for the second-stage parameters is conditional on the fixed anchor. The Hessian-based standard errors for c and $\boldsymbol{b}$ summarize uncertainty in the conditional likelihood function stated in (10), but they do not propagate uncertainty in $\widehat{\mu}_A$. Therefore, the bootstrap summaries for the anchor should be interpreted as descriptive resampling summaries for the design-based endpoint, not as ordinary confidence intervals for a regular ML-estimated location parameter.

The simulation study was intentionally boundary-calibrated. Event intervals were constructed around the latent failure times to evaluate the conditional second-stage estimation problem when the selected anchor is close to the data-generating endpoint. This design is useful for isolating the anchored likelihood behavior, but it is not a general model for naturally IC data generated by independent scheduled inspections. Future simulation studies should examine independent inspection schedules, coarser observation grids, left-censoring-dominated designs, informative visit processes, independent censoring-time distributions, and settings in which the design-based anchor differs materially from the latent lower endpoint.

The GBSG application used constructed IC observations based on assumed follow-up windows. These constructed intervals are useful for demonstrating implementation and sensitivity to window choice, but they are not a substitute for naturally IC data with recorded inspection times. Naturally IC datasets with documented visit schedules would provide a stronger empirical setting for further evaluation.

Future research may develop alternative approaches for the support endpoint, including a penalized likelihood function, profile likelihood function with regularization, and Bayesian formulations with informative or weakly informative priors. Further theoretical work is also needed to characterize the asymptotic behavior of the anchored conditional estimators under IC observation, quantify the effect of anchor choice on the shape and regression parameters, and compare anchor-based estimation with fully joint regularized methods. Extensions to time-dependent covariates, competing risks, clustered survival data, and other shifted lifetime distributions would further broaden the scope of the framework.

Appendix A: Supplementary diagnostic figures

This appendix presents the diagnostic figures corresponding to the numerical summaries reported in Tables 2-8. The figures summarize RMSE, empirical CP, and average interval-width behavior across the evaluated shape, sample-size, and censoring scenarios.

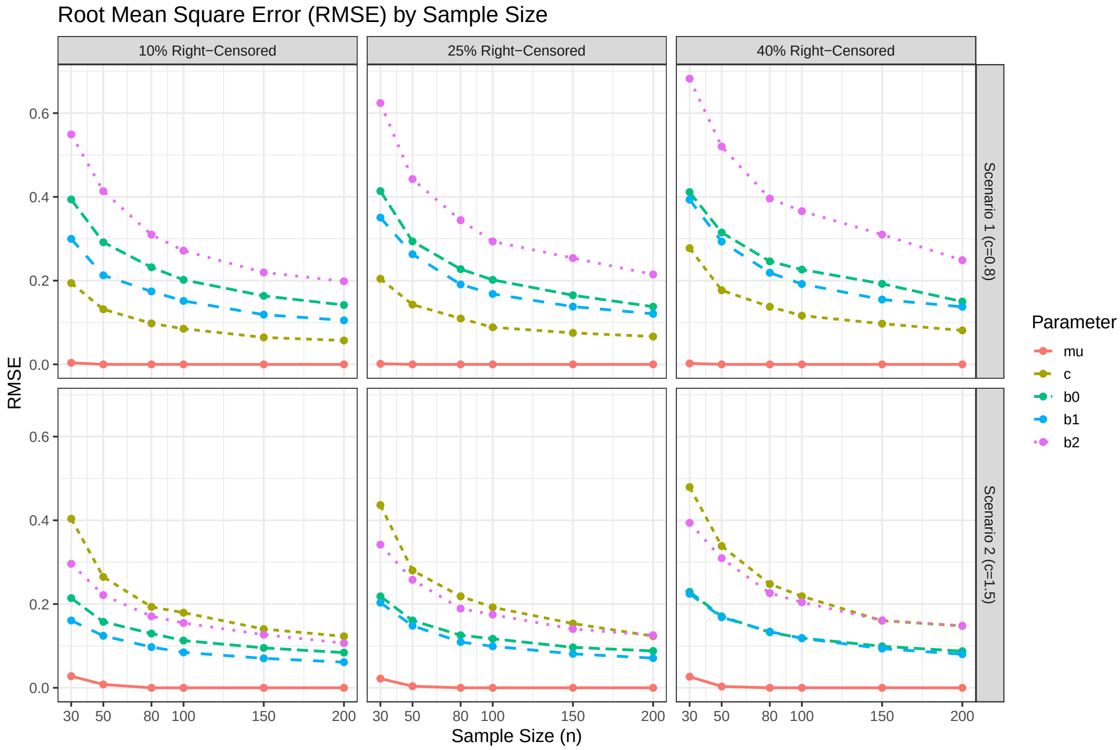

Figure 1. RMSE summaries for the boundary-calibrated diagnostic study under Scenario 1 ($c = 0.8$) and Scenario 2 ($c = 1.5$). For c, b_0, b_1, and b_2, RMSE refers to the conditional second-stage estimates. For $\widehat{\mu}_A$, RMSE refers to the design-based anchor induced by the simulated interval endpoints.

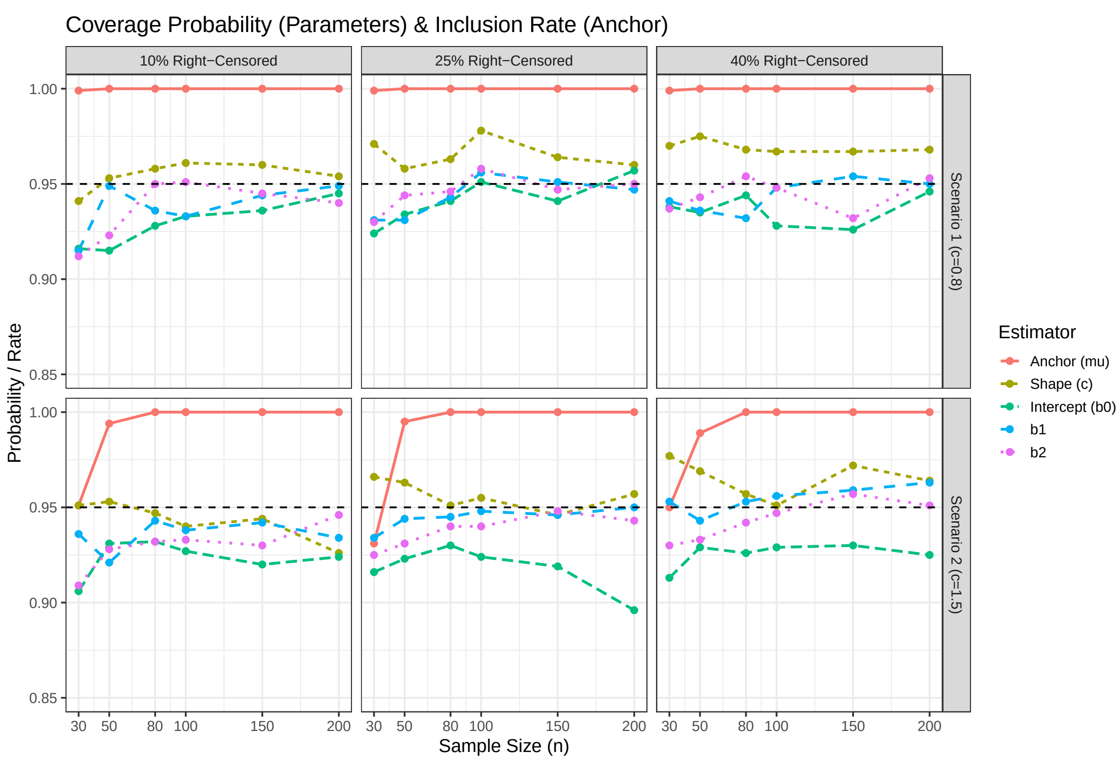

Figure 2. Empirical CP summaries for the boundary-calibrated diagnostic study under Scenario 1 ($c = 0.8$) and Scenario 2 ($c = 1.5$). For c, b_0, b_1, and b_2, values correspond to Wald intervals based on the conditional likelihood function, given the fixed anchor $\widehat{\mu}_A$. For $\widehat{\mu}_A$, the curve plots the anchor inclusion rate based on bootstrap percentile intervals, which must not be conflated with a standard confidence-interval CP for a latent location parameter.

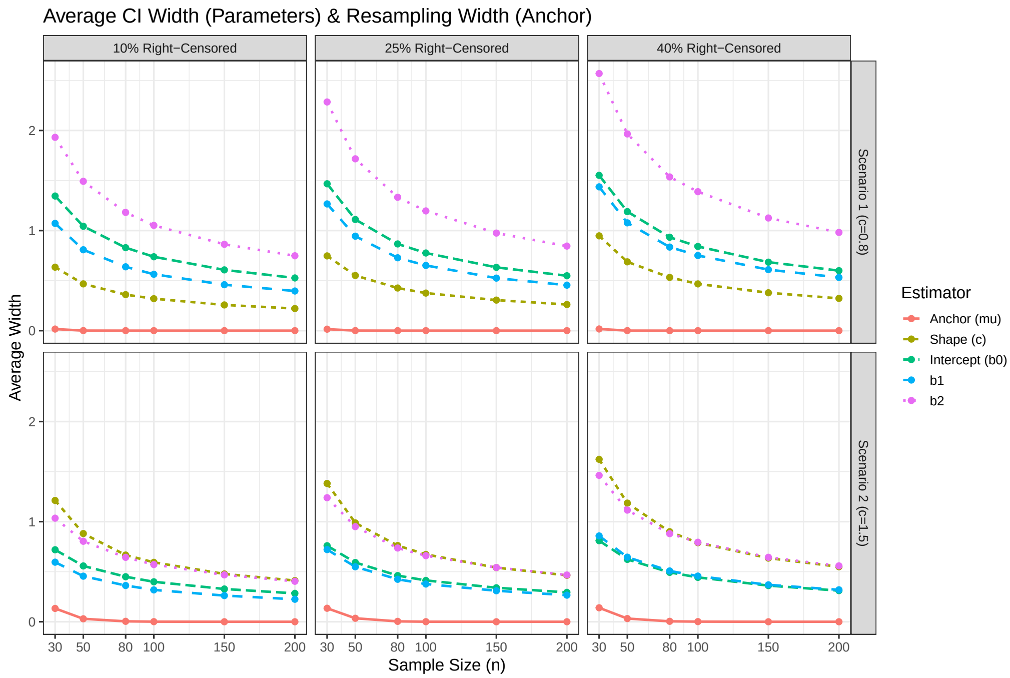

Figure 3. Average interval width summaries for the boundary-calibrated diagnostic study under Scenario 1 ($c = 0.8$) and Scenario 2 ($c = 1.5$). For c, b_0, b_1, and b_2, the ACIW is based on Wald intervals from the conditional likelihood function. For $\widehat{\mu}_A$, the curve plots the anchor resampling width and must not be interpreted as a standard confidence interval width for a latent location parameter.

Appendix B: Exact-data non-regularity and motivation

The anchor-based conditional procedure used in this article is motivated by the known non-regularity of the exact-observation three-parameter Weibull likelihood function with respect to the location parameter. These exact-data results provide useful guidance for understanding why simultaneous estimation of the location, shape, scale, and regression parameters can be numerically delicate. In this appendix, they are used as motivation for the proposed conditional strategy rather than as a direct transfer of exact-data regularity thresholds to the IC likelihood function.

For IC data, likelihood contributions are probabilities assigned to observed intervals. Therefore, the exact-data PDF singularities do not automatically imply that the IC likelihood function is unbounded. Nevertheless, the location component remains boundary-sensitive because the observed lower endpoints are determined by the inspection process. This motivates the use of the observed design-based support anchor defined in (5), followed by conditional ML estimation of the shape and regression parameters.

For exact observations from a three-parameter Weibull model, the region $c > 2$ is the regular case usually associated with standard likelihood asymptotics for the location parameter [8]. In this setting, the likelihood function is locally well behaved near the boundary, and the relevant derivatives have finite expectations under the usual regularity conditions. Consequently, standard JMLE theory can apply to the location, shape, scale, and regression parameters. In the present article, this exact-data regular case is used only as a reference point. The proposed anchor-based conditional method can still be applied when the fitted shape is greater than two, but its main practical motivation is in settings where the location component is more boundary-sensitive.

For exact observations, the PDF of the shifted Weibull model contains the factor $(t - \mu)^{c-1}$. When $0 < c < 1$, the exponent $c - 1$ is negative. As the location parameter approaches an observed failure time from below, this term can diverge.

Thus, for exact data, the likelihood function can become unbounded as μ approaches the smallest observed failure time. This is a classical source of boundary non-regularity in the three-parameter Weibull model. For IC data, the likelihood function is based on interval probabilities rather than PDF evaluations at exact event times. Hence, this exact-data unboundedness does not transfer directly to the IC likelihood function. However, when interval endpoints lie close to the boundary or when the location parameter is allowed to move toward early event intervals, the likelihood surface can still be poorly conditioned. The anchor-based strategy avoids direct optimization over this boundary-sensitive component by fixing the location at $\widehat{\mu}_A$ and optimizing only over the second-stage parameters.

The case $c = 1$ corresponds to the exponential model. For exact observations, this case is also non-regular with respect to the location parameter. The PDF is finite at the support boundary, but the support itself depends on the unknown location. As a result, standard regularity conditions for ordinary likelihood inference on the location parameter are not satisfied in the usual way. For IC data, the likelihood function is based on interval probabilities rather than exact PDF evaluations. Therefore, the exact-data non-regularity does not transfer mechanically to the IC likelihood function. Nevertheless, the location parameter remains a support parameter tied to the observed lower and upper endpoints. This provides additional motivation for treating the location component as a fixed design-based anchor in the proposed conditional analysis.

For exact observations, the likelihood function in the region $1 < c \leq 2$ is typically bounded, and a maximum may exist. However, the model remains non-regular with respect to the location parameter. The standard Fisher-information-based arguments underlying ordinary Wald inference may fail because the behavior of derivatives near the lower endpoint is not sufficiently regular. A heuristic way to see this is that second-derivative terms with respect to the location component involve powers of $t - \mu$ that can be non-integrable near the boundary when $1 < c \leq 2$. As a result, the location estimator has non-standard asymptotic behavior in exact-observation settings, and ordinary joint Wald inference for the full parameter vector is not reliable in the usual way. For IC data, the use of interval probabilities smooths the likelihood function relative to exact PDF contributions. Therefore, one should not automatically transfer the exact-data asymptotic classification to the IC setting. In this article, the exact-data result is used as a cautionary motivation: when the fitted shape lies in this region, the location component should be treated carefully, and direct joint likelihood inference may be sensitive to boundary behavior.

Our method fixes the location component at the observable design-based anchor $\widehat{\mu}_A$ and then estimates the shape and regression parameters conditionally. This removes the boundary-sensitive location component from the iterative second-stage optimization, and so the numerical search is carried out over c and $\boldsymbol{b}$, conditional on a fixed support endpoint. The piecewise likelihood function can also be evaluated without undefined terms at the boundary. When an observed lower endpoint satisfies $L_i \leq \widehat{\mu}_A$, the contribution is handled through $S(L_i) = 1$, while the right endpoint remains active in the likelihood function. The resulting estimates have a conditional interpretation. They estimate the shape and regression parameters of the anchored shifted Weibull working model, given $\widehat{\mu}_A$. They should not be described as ordinary joint ML estimates of the full latent three-parameter Weibull model. The diagnostic study evaluates this conditional framework under a boundary-calibrated data-generating mechanism. In that design, the observed event-interval lower endpoints are constructed so that the anchor is close to the true lower endpoint. Under this setting, the conditional likelihood function for the second-stage parameters is numerically stable, and the RMSE for c and $\boldsymbol{b}$ decreases with increasing sample size. Thus, the diagnostic evidence supports the conditional performance of the second-stage estimation problem when the anchor is close to the effective lower endpoint. It illustrates the design-dependent behavior of $\widehat{\mu}_A$, which is summarized separately from the ML-estimated parameters.

Appendix C: Comparison with converged constrained joint-likelihood fits

This appendix compares the proposed anchor-based conditional method with the best converged constrained joint-likelihood fit(s) for the constructed GBSG IC datasets.

These fits are referred to as constrained joint fits because the location, shape, and regression parameters are optimized simultaneously. Since the numerical optimization uses a finite number of starting values, the results should not be interpreted as guaranteed global joint ML estimates.

In the constrained joint fit, (μ, c, b_0, b_1, b_2) are optimized using the same piecewise IC likelihood structure as given in (9), but with the fixed anchor $\widehat{\mu}_A$ replaced by the free location parameter μ. The optimization is performed under the support-domain restrictions $0 \leq \mu < \min_{i:\delta_{I_i}=1}\{R_i\}$, with $c > 0$. The restriction on μ ensures that every observed event interval has a right endpoint strictly beyond the fitted support endpoint. If $\mu \geq R_i$ for any event interval, that interval would lie entirely at or before the fitted lower endpoint and its event probability would be zero under the shifted Weibull model.

The constrained joint fit was computed using five random starting values, and the best converged solution was retained. This multi-start procedure reduces sensitivity to initialization but does not guarantee that the global maximum has been found. Therefore, the comparison is numerical and descriptive rather than a proof of global optimality of the joint fit. The comparison was performed for the 10-, 20-, and 30-day constructed event-window datasets. Within each window, both methods are applied to the same constructed IC dataset. Across different windows, the interval endpoints change, and so likelihood functions should be interpreted within each window rather than as model-selection quantities across windows.

Table 13 summarizes the location values, shape estimates, and log-likelihood functions obtained by the anchor-based conditional method and the best converged constrained joint-likelihood fit(s) across the three constructed windows.

Table 13. Anchor-based conditional method and best converged constrained joint-likelihood fits across constructed GBSG interval windows.

Window	Method	Loc	$\widehat{c}$	LogLik	$\Delta\ell$	ΔLoc
10 days	Anchor-based	62.00	1.151	-1933.76	-0.19	-4.20
	joint fit	66.20	1.141	-1933.56	–	–
20 days	Anchor-based	52.00	1.160	-1728.24	-1.35	-14.39
	joint fit	66.39	1.128	-1726.89	–	–
30 days	Anchor-based	42.00	1.169	-1608.77	-2.84	-24.48
	joint fit	66.48	1.114	-1605.93	–	–

Note: For the anchor-based method, "Loc" denotes the fixed design-based anchor $\widehat{\mu}_A$. For the constrained joint fit, "Loc" denotes the jointly optimized location parameter from the best converged run among the finite set of starting values. The quantity $\Delta\ell$ is the anchor-based log-likelihood minus the constrained joint-fit log-likelihood within the same constructed window. The quantity ΔLoc is the anchor-based location value minus the constrained joint-fit location value.

The constrained joint fit attains a higher log-likelihood than the anchor-based conditional method in all three constructed windows. This is expected because the constrained joint fit optimizes over the location parameter, whereas the anchor-based method fixes the location component before estimating the shape and regression parameters. Therefore, the comparison illustrates a trade-off between optimizing the likelihood function over a larger parameter space and imposing an observed design-based support endpoint.

For the primary 10-day construction, the log-likelihood difference is small, as shown in Table 13. This indicates that, for this constructed dataset, the anchor-based fit achieves a conditional likelihood function very close to the best converged constrained joint fit while using the observable event lower endpoint as the support anchor.

As the assumed interval window widens, the anchor moves earlier by construction, while the constrained joint-fit location value remains near 66 days across the three windows. Consequently, the log-likelihood difference increases as the constructed anchor moves farther from the jointly optimized location value.

The shape estimates are also informative. The anchor-based method gives shape estimates between 1.151 and 1.169 across the three windows. The constrained joint fits give shape estimates between 1.114 and 1.141. Therefore, both approaches indicate an increasing post-location hazard under these fitted models. The anchor-based estimates vary modestly across the three constructed windows, suggesting that fixing the support endpoint can produce a stable conditional shape estimate in this application.

The two location values have different interpretations. The anchor-based value is determined directly by the constructed interval endpoints and represents the earliest observed event lower endpoint for each window. The constrained joint-fit value is obtained by numerical optimization of the likelihood function over the location parameter, conditional on the finite multi-start procedure. Thus, the anchor-based method prioritizes an observed design-based support endpoint, while the constrained joint fit prioritizes numerical likelihood fit within the specified parameter constraints.

In summary, this comparison shows that the anchor-based conditional method provides a stable and interpretable conditional fit for the constructed GBSG interval datasets. The constrained joint fits provide higher likelihood values by optimizing over the location parameter, but they are not claimed to be guaranteed global joint ML estimates. The results support the use of the anchor-based method when the analysis prioritizes a design-based support endpoint and conditional inference for the shape and regression parameters.

Appendix D: Boundary-stress illustration using the `miceData` dataset

This appendix presents a boundary-stress illustration using the `miceData` dataset [18], available in the `icenReg` package. The purpose is to compare the proposed anchor-based conditional method with a best converged constrained joint-likelihood fit(s) in a dataset containing many early IC observations with lower endpoint zero.

The dataset concerns time to tumor onset in mice, comparing conventional environment (`ce`) and germ-free environment (`ge`) groups, and contains $N = 144$ observations. A substantial fraction of the observations have lower interval endpoint $L = 0$. Such observations indicate that the event occurred before or by the first recorded upper inspection time, but they do not resolve the exact onset time within that early interval. Under the proposed method, this structure leads naturally to a design-based anchor at zero.

A shifted Weibull regression model was fitted using the treatment group indicator. To stress-test the mixed-covariate implementation, a synthetic auxiliary continuous covariate, generated from a $\mathrm{N}(25, 5^2)$ distribution and subsequently standardized using the random seed 456, was also included in the computational analysis. This auxiliary covariate is synthetic and has no biological interpretation in the original mice experiment. It is used only to verify the numerical behavior of the model with both categorical and continuous covariates. The anchor-based method fixed the location component at the observed lower-endpoint anchor and then estimated the shape and regression parameters conditionally. The constrained joint fit optimized (μ, c, b_0, b_1, b_2) simultaneously under the same piecewise likelihood function and domain restrictions. The constrained joint fit was computed using five random starting values, and the best converged solution was retained.

Table 14 reports the fitted location value, shape estimate, Hessian-based standard error for the shape parameter, and log-likelihood function for both methods.

Table 14. Boundary-stress illustration using the `miceData` dataset.

Method	Loc	$\widehat{c}$	SE ($\widehat{c}$)	LogLik	Status
Anchor-based conditional	0.0000	1.9256	0.7641	-79.6805	Converged
Constrained joint fit	265.9998	0.9714	0.4779	-79.3907	Converged at upper bound

Note: For the anchor-based method, "Loc" denotes the fixed design-based anchor $\widehat{\mu}_A = \min\{L_i\} = 0$. For the constrained joint fit, "Loc" denotes the jointly optimized location parameter from the best converged run among the finite set of starting values. The reported standard errors are Hessian-based numerical summaries. For the anchor-based method, the standard error for $\widehat{c}$ is conditional on the fixed anchor. Because the constrained joint fit reached the imposed numerical upper bound ($\min_{i:\delta_{I_i}=1}\{R_i\} - 10^{-4} = 265.9999$), ordinary interior Hessian inference is inappropriate; therefore, its reported standard error for $\widehat{c}$ must be interpreted strictly as an exploratory numerical curvature summary conditional on this active bound.

The two methods produce different fitted location values, as shown in Table 14. The anchor-based conditional method fixes the location component at zero because the dataset contains early intervals with lower endpoint zero. Conditional on this anchor, the fitted shape parameter is greater than one, corresponding to an increasing post-anchor hazard under the shifted Weibull model.

The synthetic auxiliary continuous covariate is not used to draw biological conclusions. Therefore, the scientific interpretation of this illustration is restricted to the behavior of the fitted support endpoint and shape parameter under a boundary-stress interval structure.

The constrained joint fit optimizes the location parameter simultaneously with the shape and regression parameters and reaches the imposed upper bound. In this example, the optimized location should be interpreted as a boundary-sensitive numerical joint fit rather than as a directly observed onset time. Its fitted shape parameter is close to one. Thus, the two methods describe different fitted support structures for the same coarsely observed early-event data.

The constrained joint fit achieves a small log-likelihood gain (approximately 0.29) over the anchor-based conditional method, as reported in Table 14. This marginal gain must be interpreted in a boundary-saturation context: the optimization is completely driven against the active upper-bound constraint rather than finding an interior maximum. The comparison thus reflects a trade-off between a marginal numerical joint-likelihood gain at a saturation bound and a principled design-based anchoring.

The Hessian-based standard error for the anchor-based shape estimate is interpreted conditional on the fixed anchor. The Hessian-based standard error from the constrained joint fit is a numerical summary from the joint optimization. Because the two fitted models use different location values, their shape estimates and standard errors should be interpreted within their own fitted likelihood frameworks.

This boundary-stress illustration shows how the proposed method behaves when early observations force the design-based anchor to zero. The anchor-based conditional fit estimates an increasing post-anchor hazard and keeps the support endpoint tied to the observed lower endpoints. The constrained joint fit attains a slightly higher likelihood by optimizing a later location value jointly with the shape and regression parameters. Therefore, the example illustrates the practical distinction between a design-anchored conditional fit and a likelihood-driven joint location fit in a dataset with coarse early interval information.

Statements

Acknowledgments

The authors would like to thank the editors and anonymous reviewers for their valuable comments and suggestions, which helped us significantly improve the quality of this article.

Author contributions

Conceptualization: S. Kapoor. Data curation: S. Kapoor. Formal analysis: S. Kapoor. Investigation: S. Kapoor. Methodology: S. Kapoor. Software: S. Kapoor. Supervision: A. Gupta. Validation: A. Gupta. Visualization: S. Kapoor. Writing—original draft: S. Kapoor. Writing—review and editing: S. Kapoor and A. Gupta. All authors have read and approved the final version of the article.

Conflicts of interest

The authors declare no conflict of interest.

Data and code availability

The GBSG dataset used in Section 5 is available through the R package `shrink`. The `miceData` dataset used in Appendix D is available through the R package `icenReg`. The simulation datasets are generated by the supplied Monte Carlo script.

All simulations and data analyses were performed in the R programming environment [17]. Data manipulation and formatting were carried out using the `dplyr` and `tidyr` packages. Optimization was conducted using the `optim` function from the base `stats` package with the L-BFGS-B algorithm. Code Availability: All R scripts required to generate the simulated datasets, perform the estimations, and produce the reported tables and figures are available at github.com/skapoor-scholar/GWM_Interval-Censor_Final.

Execution Map: The reported outputs can be reproduced from the supplied scripts, subject to the recorded software versions and package dependencies.

- `Script_1_Simulation.R`: Generates the Monte Carlo simulation datasets, fits the anchor-based conditional Generalized Weibull model, and outputs the performance metrics (RMSE, empirical CP, ACIW, convergence rates, variance validity, and optimization penalties). Appendix A, Figures 1, 2, and 3, and Tables 2–8.
- `Script_2_GBSG_Analysis.R`: It loads the GBSG dataset via the `shrink` package, constructs the IC representations under the 10-, 20-, and 30-day windows, fits the anchored GWM and two-parameter Weibull comparison, and outputs Tables 9, 10, 11, and 12.
- `Script_3_Appendix_C_JMLE.R`: It executes the multi-start comparison between the anchor-based conditional method and the best converged constrained joint-likelihood fit(s), outputting Table 13.
- `Script_4_Appendix_D_MICE.R`: It loads the `miceData` dataset from the `icenReg` package, constructs the boundary-stress illustration with the treatment indicator and seeded synthetic auxiliary continuous covariate, and outputs Table 14.

All scripts include explicit random seeds and `sessionInfo()` output to support reproducibility.

Declaration on the use of artificial intelligence (AI) technologies

The authors used a generative AI tool for language refinement and assistance with R-code debugging. The authors take full responsibility for the statistical methodology, computations, interpretations, and final content of the article.

Funding

This work did not receive any specific grant from funding agencies in the public, commercial, or not-for-profit sectors.

References

[1] Collett, D., 2023. Modelling Survival Data in Medical Research. Chapman and Hall/CRC, Boca Raton, FL, US. DOI: 10.1201/9781003282525.

[2] Azevedo, M., Meira-Machado, L., and Moreira, C., 2025. Non-Markov multi-state survival analysis with complex censoring: A structured synthesis of models, estimators, and applications. Chilean Journal of Statistics, 16, 125–177. DOI: 10.32372/ChJS.16-02-02.

[3] Klein, J.P. and Moeschberger, M.L., 2003. Survival Analysis: Techniques for Censored and Truncated Data. Springer, New York, NY, US. DOI: 10.1007/b97377.

[4] Zhang, Z. and Sun, J., 2010. Interval censoring. Statistical Methods in Medical Research, 19, 53–70. DOI: 10.1177/0962280209105023.

[5] Turnbull, B.W., 1974. Nonparametric estimation of a survivorship function with doubly censored data. Journal of the American Statistical Association, 69, 169–173. DOI: 10.1080/01621459.1974.10480146.

[6] Lai, C.D., 2014. Generalized Weibull Distributions. Springer, Heidelberg, Germany. DOI: 10.1007/978-3-642-39106-4.

[7] Kundu, D. and Raqab, M.Z., 2009. Estimation of $R = P(Y < X)$ for the three-parameter Weibull distribution. Statistics and Probability Letters, 79, 1839–1846. DOI: 10.1016/j.spl.2009.05.026.

[8] Cheng, R.C.H. and Iles, T.C., 1987. Corrected maximum likelihood in non-regular problems. Journal of the Royal Statistical Society B, 49, 95–101. DOI: 10.1111/j.2517-6161.1987.tb01430.x.

[9] Sauerbrei, W., Royston, P., Bojar, H., Schmoor, C., and Schumacher, M., 1999. Modelling the effects of standard prognostic factors in node-positive breast cancer. British Journal of Cancer, 79, 1752–1760. DOI: 10.1038/sj.bjc.6690279.

[10] Keret, N. and Gorfine, M., 2023. Analyzing big EHR data—optimal Cox regression subsampling procedure with rare events. Journal of the American Statistical Association, 118, 2262–2275. DOI: 10.1080/01621459.2023.2209349.

[11] Brunel, E., Comte, F., and Guilloux, A., 2009. Nonparametric density estimation in presence of bias and censoring. TEST, 18, 166–194. DOI: 10.1007/s11749-007-0075-5.

[12] Shen, P.S., 2022. Nonparametric analysis of doubly truncated and interval-censored data. Statistical Methods in Medical Research, 31, 1157–1170. DOI: 10.1177/09622802221084133.

[13] Rossi, P.E., 2014. Bayesian Non- and Semi-parametric Methods and Applications. Princeton University Press, Princeton, NJ, US. DOI: 10.1515/9781400850303.

[14] Alharbi, N., Arasan, J., Abd Rahman, N.H., and Ling, W., 2022. Assessing performance of the generalized exponential model in the presence of the interval censored data with covariate. Austrian Journal of Statistics, 51, 52–69. DOI: 10.17713/ajs.v51i1.1192.

[15] Al-Hakeem, H.A., Arasan, J., Bin Mustafa, M.S., and Peng, L.F., 2023. Parameter estimation for the generalized exponential distribution in the presence of interval censored data and covariate. International Journal of Nonlinear Analysis and Applications, 14, 739–751. DOI: 10.22075/ijnaa.2021.23746.2607.
[16] Salem, H.M. and Selim, M.A., 2014. The generalized Weibull–exponential distribution: Properties and applications. International Journal of Statistics and Applications, 4, 102–112. DOI: 10.5923.j.statistics.20140402.04.
[17] R Core Team, 2023. R: A Language and Environment for Statistical Computing. R Foundation for Statistical Computing, Vienna, Austria. URL: www.R-project.org.
[18] Hoel, D.G. and Walburg, H.E., Jr., 1972. Statistical analysis of survival experiments. Journal of the National Cancer Institute, 49, 361–372. DOI: 10.1093/jnci/49.2.361.